PERFORMANCES OF PACKED BED DOUBLE PASS SOLAR AIR HEATER WITH DIFFERENT INCLINATIONS AND TRANSVERSE WIRE MESH WITH DIFFERENT INTERVALS

by

Sam Stanley SUGANTHARAJ GNANADURAI [a]***, Anbarasan VIJAY KUMAR*** [b]***, and Kalidasa Murugavel KULUNDAIVEL*** [b]

[a] Department of Mechanical Engineering, PARK College of Engineering and Technology, Coimbatore, Tamil Nadu, India
[b] Centre for Energy Studies, National Engineering College, K. R. Nagar, Kovilpatti, Tamil Nadu, India

Original scientific paper
DOI: 10.2298/TSCI131015085S

Solar air heating is a technology in which the solar energy from the sun is captured by an absorbing medium and used to heat the air flowing through the heater. In this study, thermal performance of a double pass solar air heater has been investigated experimentally at different conditions. The experiments were conducted with different inclinations of the collector, with and without wire mesh vertically fixed at the second pass in transverse direction and with different mass flow rates. The effect of air mass flow rate, wire mesh pitch and collector inclination on temperature rise and thermal efficiency have been studied. Results show that efficiency increases with mass flow rate. For the same mass flow rate, the thermal efficiency increases with the decrease in the wire mesh pitch. The maximum daily average efficiency of air heater was 79.8% at 0.025 kg/s mass flow rate, 10 cm wire mesh gap and 9° collector inclination facing south. The highest collector efficiency was observed in solar air heaters with 10 cm wire mesh gap.

Key words: *solar air heater, packed bed, porous media, wire mesh*

Introduction

Solar air heaters (SAH) are extensively used for space heating, drying agricultural products such as fruits, seeds and vegetables and industrial processes. The SAH absorber plate receives solar radiation through transparent cover, convert the radiation into heat, and transfer it to flowing air over it. During this process, some heat is lost through the cover into atmosphere. Hence, the heater performance mainly depends on the heat transfer coefficient between the absorber plate and flowing air and the convection heat loss through the glass cover. Numbers of attempts were made to minimize the convection heat loss through the top glass cover. Sachunanathan and Deonarine [1] used double-glazing to suppress the convection loss through frontal cover and concluded that smaller gap between these glasses yielded better result. Mohamad [2] claimed that preheating the air by passing air through the gap between the covers improved the heater efficiency. Flowing of air simultaneously above and below the absorber

* Corresponding author; e-mail: kali_vel@rediffmail.com, hodces@nec.edu.in

plate [3, 4] improved the performance of the heater. Yeh *et al*. [5] used same area of cross-section and mass flow rate for upper and lower section of the double flow air heater to get maximum efficiency. Flowing air first over and then below the absorber plate improved the efficiency further [6, 7]. Jain and Jain [8] presented study on multi pass air heater with double-glazing. In this study, the air was initially passed through the gap between the glasses and then through upper section between the glass and absorber plate and finally through the lower section below the absorber plate. Different modifications were suggested and implemented to increase the area of contact between the air and absorber plate. Absorber plate with different roughness geometries [9, 10] has higher heat transfer characteristics compared with that of smooth surface. When airflow occurs through porous medium in flow section, the heat transfer is enhanced due to increase in contact area [10, 11]. Sopian *et al.* [12] investigated the thermal performance of a double-pass solar collector and concluded that the presence of porous media in the second channel increased the outlet temperature and thermal efficiency of the systems. Phase change materials packed in capsules were used in air heaters as obstacles and to store excess energy [13]. Krishananth and Murugavel [14] studied the performance of a double pass air heater with phase change energy storing material capsules in different locations and concluded that, placement of capsules on the absorber plate was more effective. Mittal and Varshney [15] compared the performance of the air heater packed with wire mesh for different geometrical parameters and suggested to select a matrix which would result in best thermal performance with minimum pressure loss. Prasad *et al*. [16] investigated the performances of air heater with eight different wire mesh packed bed configurations. The efficiency increased with mass flow rate up to a typical value, beyond which the increase was insignificant. Aldabbagh *et al.* [17] obtained a maximum thermal efficiency of 83.65% by using a porous media instead of an absorber plate in the double pass model. El-Khawajah *et al*. [18] reached 85.9% efficiency by using six transverse fins. Omojaro and Aldabbagh [19] observed that, reducing the upper channel height increased the thermal performance. Yousef-Ali [20] optimized the thermal performances of the offset rectangular plate fin absorber plates, with various glazings. Walid Aissa *et al*. [21] studied the performance of forced convection air heater with granite stone storage material. It was concluded that air mass flow rate and solar radiation are the predominant factors affecting the performance of air heaters. Energy and exergy studies were conducted [22] on solar air collectors and was suggested that, among the tested mass flow rates, a mass flow of 0.0011 kg/s was the optimum. Obstacles placed in the air vein [23] improved the thermal exchange between the air and the absorber. In this study, the performance of a counter flow double pass solar air heater has been experimentally analyzed and compared for various bed conditions. Experiments have been carried out with various inclinations of the collector (β), collectors without wire mesh, and collectors with wire meshes at gaps (g) of 10 cm, 12 cm, and 14 cm. The performance of the air heater has been studied for various mass flow rates such as 0.025 kg/s, 0.020 kg/s, 0.015 kg/s, and 0.010 kg/s.

Experimental

The counter flow two pass solar air heater was fabricated as shown in fig. 1 and tested at the Energy park of National Engineering College, Kovilpatti (9°11' N, 77°52' E), India. The 150 cm × 100 cm collector with two flow sections separated by absorber plate was fabricated using 1 mm thick mild steel plate. The interior sides were black painted and outer sides were insulated using 3 cm thick thermocol. In the lower flow section, 100 cm × 7 cm × 0.1 cm size aluminum wire meshes were fixed vertically as shown in fig. 2. To ensure uniform flow through entire area of the heater, conical inlet and exit sections were employed. A blower was used to suck the

Figure 1. Set-up of double pass SAH, with vertically arranged wire mesh
1 – adjustable vertical stand, 2 – glass cover, 3 – insulation, 4 – air inlet, 5 – air outlet, 6 – U tube manometer, 7 – blower, 8 – control valve

air from lower section through a venturimeter and control valve. In order to investigate the effect of various parameters on the performance of the SAH, experiments were performed outdoor during March 2012 with different mass flow rates of air, various tilt angles of the collector and by varying the gap between the wire meshes placed vertically in the collector. A water differential manometer was connected to venturi meter to measure the airflow and the control valve was used to adjust the airflow. Provisions were made to insert K-type thermo couple to measure the air inlet and exit temperatures, absorber plate temperature, and wire mesh temperature. Calibrated mercury type thermometer was used to read atmospheric temperature and PV-type radiation meter was used to measure the solar intensity on the inclined glass cover. Experiments were conducted in SAH at actual solar condition. First experiment was conducted by varying the gap between wire mesh. The readings were taken for different mass flow rate in the range of (0.01-0.025 kg/s). Second experiment was conducted by changing the collector set-up angle in the vertical stand, different tilt angles (9°, 20°, and 25°). The readings were taken for the same mass flow rates. Experiment was also conducted in solar air heater with no wire mesh in the collector.

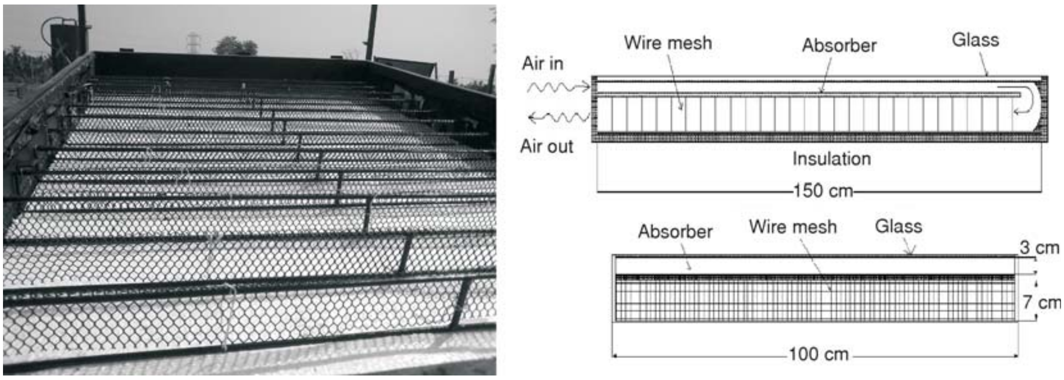

Figure 2. Photographic and schematic view of wire mesh arrangement in SAH

Uncertainty analysis of mass flow rate and efficiency

The uncertainty due to mass flow rate and thermal efficiency has to be dealt with. The uncertainties for the flow measurement through the venturi meter may have the collective effect on the mass flow rate due to uncertainty in the measurement of coefficient of discharge, measurement of area, measurement of the inlet and outlet pressures and measurement of inlet temperature. The flow rate is a function of several variables, each subject to an uncertainty. The basic relation describing the flow rate, neglecting the area ratio between upstream and downstream for calculation of uncertainty as presented by Holman [24] for the determination of uncertainty in the mass flow rate by including the collective effects of absolute pressure p_1, gas constant R, and temperature of air T_{1u} is given by:

$$\dot{m} = A_{\mathrm{u}} C_{\mathrm{d}} \sqrt{2 \frac{p_1}{\mathrm{R} T_{1\mathrm{u}}} (p_1 - p_2)} \tag{1}$$

$$\dot{m} = f(C_{\mathrm{d}}, A_{\mathrm{u}}, p_1, \Delta p, T_{1\mathrm{u}}) \tag{2}$$

Thus, forming the derivatives:

$$\frac{\partial \dot{m}}{\partial C_{\mathrm{d}}} = A_{\mathrm{u}} \sqrt{\frac{2 g_{\mathrm{c}} p_1}{\mathrm{R} T_{1\mathrm{u}}} \Delta p} \tag{3}$$

$$\frac{\partial \dot{m}}{\partial A_{\mathrm{u}}} = C_{\mathrm{d}} \sqrt{\frac{2 g_{\mathrm{c}} p_1}{\mathrm{R} T_{1\mathrm{u}}} \Delta p} \tag{4}$$

$$\frac{\partial \dot{m}}{\partial p_1} = 0.5 C_{\mathrm{d}} A_{\mathrm{u}} \sqrt{\frac{2 g_{\mathrm{c}} p_1}{\mathrm{R} T_{1\mathrm{u}}} \Delta p} \frac{1}{\sqrt{p_1}} \tag{5}$$

$$\frac{\partial \dot{m}}{\partial \Delta p} = 0.5 A_{\mathrm{u}} \sqrt{\frac{2 g_{\mathrm{c}} p_1}{\mathrm{R} T_{1\mathrm{u}}}} \frac{1}{\sqrt{\Delta p_1}} \tag{6}$$

$$\frac{\partial \dot{m}}{\partial T_1} = -0.5 C_{\mathrm{d}} A_{\mathrm{u}} \sqrt{\frac{2 g_{\mathrm{c}} p_1}{\mathrm{R} T_{1\mathrm{u}}} \Delta p} \frac{1}{T_{1\mathrm{u}}^3} \tag{7}$$

Let W_{R} be the uncertainty in the result and W_1, W_2, ... W_{n} be the uncertainties in the independent variables. Uncertainty in the result having these odds is given as:

$$W_R = \sqrt{\left(\frac{\partial R}{\partial x_1} W\right)^2 + \left(\frac{\partial R}{\partial x_2} W_2\right)^2 + \cdots + \left(\frac{\partial R}{\partial x_{\mathrm{n}}} W_{\mathrm{n}}\right)^2} \tag{8}$$

The uncertainty in the mass flow may now be calculated by assembling these derivatives in accordance with the above equation designating this equation:

$$\frac{\omega_{\dot{m}}}{\dot{m}} = \sqrt{\left(\frac{\omega_{\mathrm{C_d}}}{C_{\mathrm{d}}}\right)^2 + \left(\frac{\omega_{A_u}}{A_{\mathrm{u}}}\right)^2 + \frac{1}{4}\left(\frac{\omega_{\mathrm{p_1}}}{p_1}\right)^2 + \left(\frac{\omega_{\Delta p}}{\Delta p}\right)^2 + \left(\frac{\omega_{T_{1u}}}{T_{1\mathrm{u}}}\right)^2} \tag{9}$$

By taking into assumption that uncertainty exists only in the measurement of pressure difference and the measurement of temperature, the above mentioned equation reduces, giving the uncertainty in the mass flow rate [23]:

$$\frac{\omega_{\dot{m}}}{\dot{m}} = \sqrt{\left(\frac{\omega_{\Delta p}}{\Delta p}\right)^2 + \left(\frac{\omega_{\mathrm{T_1}}}{T_{1\mathrm{u}}}\right)^2} \tag{10}$$

The mean average values for $T_{1\mathrm{u}}$, m, I, and η were found to be 305.36 K, 0.0175 kg/s, 571 W/m^2, and 42.70, respectively. Uncertainty of mass flow rate is determined as 2.95%. The efficiency of the solar collector, η, is defined as the ratio of energy gain to solar radiation incident on the collector plate:

$$\eta = \frac{\dot{m} c_p (T_2 - T_1)}{IA} \tag{11}$$

Uncertainty of efficiency is given by the following equation as stated in the work by Omojoro and Aldabbagh [19] and is determined as 5.6 %.

$$\frac{\omega_\eta}{\eta} = \sqrt{\left(\frac{\omega_{\dot{m}}}{\dot{m}}\right)^2 + \left(\frac{\omega_{\Delta T}}{\Delta T}\right)^2 + \left(\frac{\omega_{\mathrm{I}}}{I}\right)^2} \tag{12}$$

The fractional uncertainty of the mass flow rate and the efficiency are found to be 0.0295 and 0.056, respectively.

Results and discussions

The experiments were conducted under Kovilpatti Weather conditions during March 2012. The experiments were conducted with SAH without wire mesh, SAH with 10 cm wire mesh, SAH with 12 cm wire mesh and SAH with 14 cm wire mesh. Collector tilt angles were varied as 9°, 20°, and 25° and mass flow rates were varied as 0.025 kg/s, 0.020 kg/s, 0.015 kg/s, and 0.010 kg/s. The fractional uncertainty of the mass flow rate and efficiency are found to be 0.0295 and 0.056, respectively. Figure 3. Shows the variation of solar intensity during which the experiments are conducted with modification of wire mesh gap as 10 cm with angle of inclination of the collector being 25°. The other collector tilt angles fixed for experimentation was 9° and 20°. The solar intensity was found to increase from morning to noon and then it was found to have a decline till evening. It was the same phenomenon for 12 cm, 14 cm and no wire mesh. But this phenomenon had exceptions during some days because of change in weather conditions. The average solar intensities were 555.17 W/m^2, 547.88 W/m^2, and 544.43 W/m^2 with 10 cm, 12 cm, and 14 cm wire mesh gaps, respectively. The hourly variation of atmospheric temperature on the days during which experiments were carried out with the wire mesh gap of 10 cm, with different mass flow rates and with a collector tilt angle of 25° is shown in fig. 4. As expected, temperature was found to increase from morning to noon and has a decrease from noon to evening. When experiments were conducted with SAH having no wire mesh, 12 cm wire mesh and 14 cm wire mesh the same above mentioned phenomena was observed. The highest atmospheric temperature of 38 °C was reported at one instant at mass flow rate of 0.020 kg/s with 14 cm wire mesh, 9° inclination. The average atmospheric temperatures were 32.40 °C, 32.49 °C, and 32.50 °C for 10 cm, 12 cm, and 14 cm wire mesh SAH, respectively.

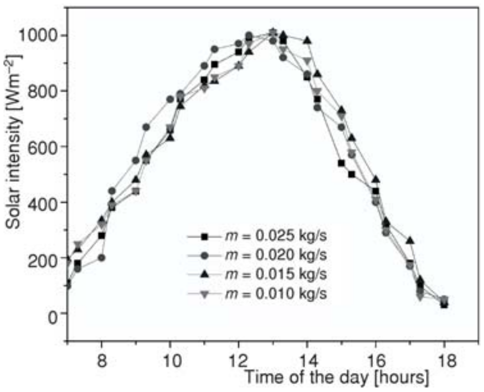

Figure 3. Hourly variation of solar intensity *vs.* different standard local time for 10 cm wire mesh gap with collector tilt angle of 25°

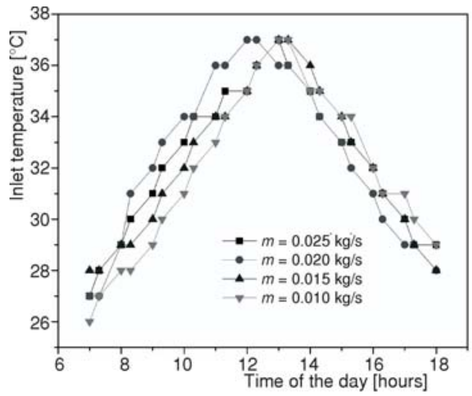

Figure 4. Hourly variation of inlet temperature *vs.* different standard local time for 10 cm wire mesh gap 25° inclination collector angle

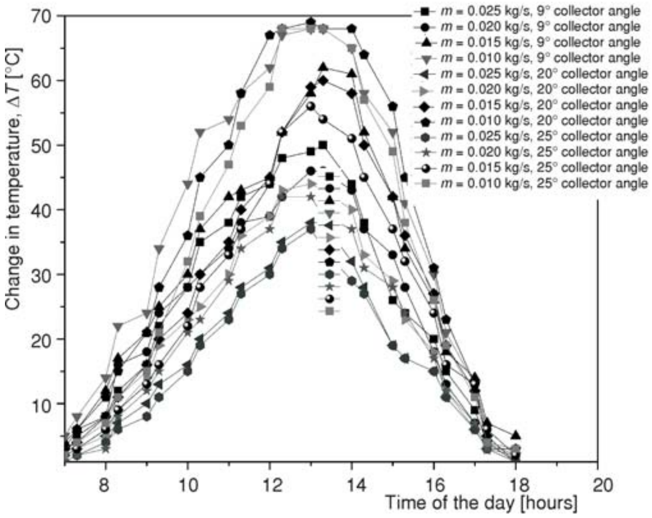

Figure 5. Temperature difference *vs.* standard local time of the day at different mass flow rates for 10 cm wire gap mesh SAH

The hourly temperature difference ($\Delta T = T_2 - T_1$) at different mass flow rates for 10 cm wire mesh gap is shown in fig. 5. The temperature differences observed in 12 cm wire mesh gap, 14 cm wire mesh gap and no wire mesh SAH were lower than the temperature difference in 10 cm wire mesh SAH. As expected, for all cases the ΔT increases in the morning to a peak value at noon and starts to decrease in the afternoon. For the configuration of the solar air heater change in temperature ΔT increases with decrease in mass flow rate. It is also observed that change in temperature ΔT increases with decrease in the wire mesh gap. It is also noted that the SAH with collector angles 9° and 25° had low temperature difference than the SAH with collector angle 20°. The highest average and instantaneous peak ΔT obtained from this work were 38 °C and 69 °C, respectively, for the 10 cm wire mesh SAH with mass flow rate of 0.010 kg/s. In the experimental work by Sharma *et al.* [25], using iron chips as a packed bed, the maximum temperature difference observed was 26 °C for air mass flow rate of 0.0105 kg/s. In the meanwhile, there was a temperature difference of 33.7 °C while copper chips were used [26] as packed bed instead of iron chips. The temperature difference observed in the earlier studies by Esen [3], Sopian *et al.* [12], Ramadan *et al.* [6] and El-Sebaii *et al.* [7] were 23 °C, 40 °C, 35 °C, and 48 °C for a maximum flux of 880 W/m^2, 950 W/m^2, 850 W/m^2, and 850 W/m^2, respectively.

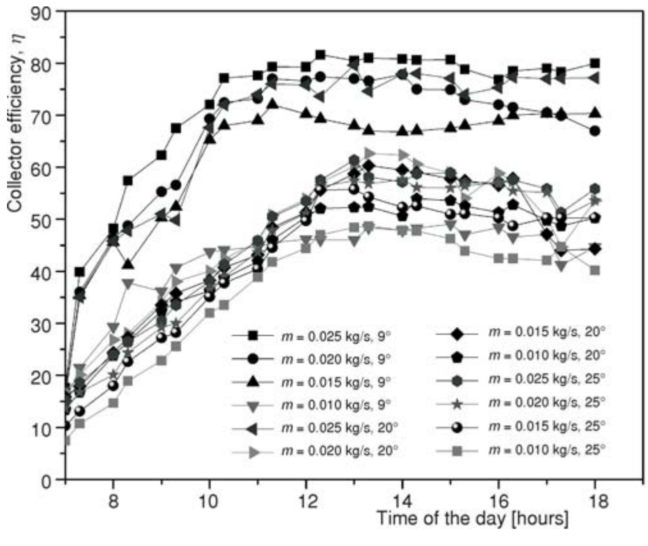

Figure 6. Variations of collector efficiency at different mass flow rates for 10 cm wire mesh with different collector angles SAH

The variations of collector efficiency for 10 cm wire mesh SAH with different mass flow rates and different collector angles is shown in fig. 6. The highest collector efficiency was observed in SAH with 10 cm wire mesh gap with collector tilt angle of 9° and mass flow rate was 0.025 kg/s. The efficiency was 81.62% at 12.30 hours during which solar Intensity was 985 W/m^2. It is interesting to note that for the same wire mesh gap SAH, and for the same mass flow rate, efficiency decreases for collector angles 20° and 25°. Hence the optimum collector angle is 9°. Also for other mass flow rates such as 0.020 kg/s, 0.015 kg/s, and 0.010 kg/s, the efficiency had a steep fall for the same configuration of SAH. The 10 cm wire mesh SAH is observed with more collector efficiency than the SAH with 12 cm wire mesh, 14 cm wire mesh, and SAH without wire mesh. It is stated here in a nutshell that collector efficiency increases with increase in mass flow rate. Between 08 and 12 hours of observation, the collector efficiency had a steady increase starting from 10% at 6.00 hours; thereby steadily increasing up to 12 Noon, Hence it may be concluded that collector efficiency is low in the morning hours. The reason for this may be due to low solar intensity during the morning hours and reduced change in temperature observed during the morning hours.

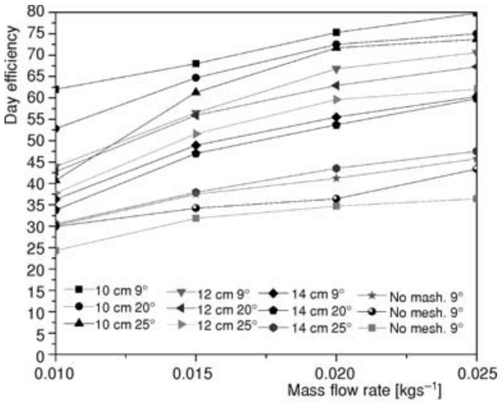

Figure 7. Average daily efficiency *vs.* mass flow rate for 10, 12, 14 and no wire mesh SAH with different collector angles

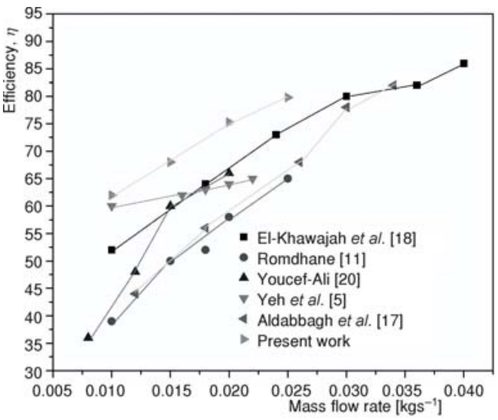

Figure 8. Comparison of efficiency of 10 cm wire mesh gap SAH with some previous work in the literature

The day efficiency (η_d) *vs.* mass flow rate for 10, 12, 14, and no wire mesh SAH with different collector angles 9°, 20°, and 25° is shown in fig. 7. The day average efficiency increases with increase in mass flow rate. The highest daily average efficiency of 79.8% was attained by SAH with 10 cm wire mesh gap, having a collector angle of 9° for a mass flow rate of 0.025 kg/s. The next highest daily average efficiency of 75.3% was attained by SAH with 10 cm wire mesh gap, having a collector angle of 9° for a mass flow rate of 0.020 kg/s. It is also observed that the SAH with collector angle 9° had more daily average efficiency than the SAH with collector angle 20° and SAH with collector angle 25°.

The comparison of day efficiency of 10 cm wire mesh gap SAH with some of SAH in the literature is shown in fig. 8. The main observation being made is that the present SAH can be more efficient for even lower mass flow rates such as 0.01 kg/s. It is also observed that for other mass flow rates the efficiency obtained is good compared with other works in the literature.

Conclusions

Performance results of double pass vertically arranged wire mesh solar air heater with and without wire mesh in lower pass have been obtained. These include the effect of mass flow rate, varying the wire mesh gap and collector tilt angle on the efficiency of solar air heater. Introducing wire mesh in the second pass increases the heat transfer area. The obtained results show that the thermal efficiency increases with increasing mass flow rate of air, between 0.01 kg/s and

0.025 kg/s. In addition to that, for 9° collector tilt angle maximum efficiency was obtained. The maximum average daily efficiency of the proposed SAH reached was around 79.8% at mass flow rate of 0.025 kg/s for 10 cm wire mesh gap with 9° collector tilt angle.

Nomenclature

A – collector area, [m^2]
A_u – area of flow in venturi meter for uncertainty determination, [m^2]
C_d – coefficient of discharge of the venturi meter, [–]
g – wire mesh gap, [cm]
g_c – acceleration due to gravity, [ms^{-2}]
I – global solar radiation on a horizontal surface, [Wm^{-2}]
$\dot{m}$ – mass flow rate of air, [kgs^{-1}]
p_1 – pressure at inlet of venturi meter, [Nm^{-2}]
p_2 – pressure at outlet of venturi meter, [Nm^{-2}]
Δp – change in pressure, [Nm^{-2}]
R – gas constant, [Jkg^{-1}K^{-1}]
ΔT – change in temperature, [°C]
T_{1u} – inlet temperature of the air-for uncertainty measurement, [K]
T_1 – inlet temperature of the air, [°C]
T_2 – outlet temperature of the air, [°C]
W_R – uncertainty of entire result, [–]

Greek symbols

β – collector tilt angle, [°]
η – collector efficiency, [–]
η_d – day efficiency, [–]
ω_{C_d} – error of coefficient of discharge of the venturi meter, [–]
ω_I – error in the measurement of solar radiation, [Wm^{-2}]
ω_{Au} – error in the measurement of area, [m^2]
$\omega_{\Delta T}$ – error in the measurement of change in temperature, [°C, K]
ω_m – uncertainty in mass flow rate, [–]
ω_η – uncertainty in efficiency, [–]

Acronym

SAH – solar air heater

References

[1] Sachunanathan, S., Deonarine, S., A Two-Pass Solar Air Heater, *Solar Energy, 15* (1973), 1, pp. 41-49
[2] Mohamad, A. A., High Efficiency Solar Air Heater, *Solar Energy, 60* (1997), 2, pp. 71-76
[3] Esen, H., Experimental Energy and Exergy Analysis of a Double-Flow Solar Air Heater Having Different Obstacles on Absorber Plates, *Build Environ, 54* (2008), 6, pp. 1046-1054
[4] Ozgen, F., *et al.*, Experimental Investigation of Thermal Performance of a Double-Flow Solar Air Heater Having Aluminium Cans, *Renewable Energy, 34* (2009), 11, pp. 2391-2398
[5] Yeh, H. M., *et al.*, Collector Efficiency of Double-Flow Solar Air Heaters with Fins Attached, *Energy, 27* (2002), 8, pp. 715-727
[6] Ramadan, M. R. I., *et al.*, Thermal Performance of a Packed Bed Double-Pass Solar Air Heater, *Energy, 32* (2007), 8, pp. 1524-1535
[7] El-Sebaii, A. A.-A., *et al.*, Year Round Performance of Double Pass Solar Air Heater with Packed Bed, *Energy Convers Manage, 48* (2007), 3, pp. 990-1003
[8] Jain, D., Jain, R. K., Performance Evaluation of an Inclined Multi-Pass Solar Air Heater with In-Built Thermal Storage on Deep-Bed Drying Application, *J Food Eng, 65* (2004), 4, pp. 497-509
[9] Gupta, M. K., Kaushik, S. C., Performance Evaluation of Solar Air Heater for Various Artificial Roughness Geometries Based on Energy, Effective and Exergy Efficiencies, *Renewable Energy, 34* (2009), 3, pp. 465-476
[10] Varun, G., *et al.*, Performance Prediction of Solar Air Heater Having Roughened Duct Provided with Transverse and Inclined Ribs as Artificial Roughness, *Renewable Energy, 34* (2009), 12, pp. 2914-2922
[11] Romdhane, B. S., The Air Solar Collectors: Comparative Study, Introduction of Baffles to Favor the Heat Transfer, *Solar Energy, 81* (2007), 1, pp. 139-149
[12] Sopian, K., *et al.*, Evaluation of Thermal Efficiency of Double-Pass Solar Collector with Porous-Nonporous Media, *Renewable Energy, 34* (2009), 3, pp. 640-645
[13] Tyagi, V. V., *et al.*, Review on Solar Air Heating System with and without Thermal Energy Storage System, *Renewable and Sustainable Energy Reviews, 16* (2012), 4, pp. 2289-2303
[14] Krishnananth, S. S., Murugavel, K. K., Experimental Study on Double Pass Solar Air Heater with Thermal Energy Storage, *Journal of King Saud University – Engineering Sciences, 25* (2013), 2, pp. 135-140

[15] Mittal, M. K., Varshney, L., Optimal Thermal-Hydraulic Performance of a Wire Mesh Packed Bed Solar Air Heater, *Solar Energy, 80* (2006), 9, pp. 1112-1120
[16] Prasad, S. B., *et al.*, Investigation of Heat Transfer and Friction Characteristics of Packed Bed Solar Air Heater Using Wire Mesh as Packing Material, *Solar Energy, 83* (2009), 5, pp. 773-783
[17] Aldabbagh, L. B. Y., *et al.*, Single and Double Pass Solar Air Heaters with Wire Mesh as Packing Bed, *Energy, 35* (2010), pp. 3783-3787
[18] El-Khawajah, M. F., *et al.*, The Effect of Using Transverse Fins on a Double Pass Flow Solar Air Heater Using Wire Mesh as an Absorber, *Solar Energy, 85* (2011), 9, pp. 1479-1487
[19] Omojaro, A. P., Aldabbagh, L. B. Y., Experimental Performance of Single and Double Pass Solar Air Heater with Fins and Steel Wire Mesh as Absorber, *Applied Energy, 87* (2010), 12, pp. 3759-3765
[20] Youcef-Ali, S., Study and Optimization of the Thermal Performances of the Offset Rectangular Plate Fin Absorber Plates, with Various Glazing, *Renewable Energy, 30* (2005), 2, pp. 271-280
[21] Aissa, W., *et al*., An Experimental Investigation of Forced Convection Flat Plate Solar Air Heater with Storage Material, *Thermal Science, 16* (2012), 4, pp. 1105-1116
[22] Mohseni Languri, E., *et al.*, An Energy and Exergy Study of a Solar Thermal Air Collector, *Thermal Science, 13* (2009), 1, pp. 205-216
[23] Saim, R., *et al*., Computational Analysis of Transient Turbulent Flow and Conjugate Heat Transfer Characteristics in a Solar Collector Panel with Internal, Rectangular Fins and Baffles, *Thermal Science, 14* (2010), 1, pp. 221-234
[24] Holman, J. P., Experimental Methods for Engineers, McGraw-Hill, New York, USA, 1989
[25] Sharma, V. K., *et al*., Design and Development of a Matrix Type Solar Air Heater, *Energy Conversion and Management, 31* (1991), 4, pp. 379-388
[26] Singh, D., *et al*., Thermal Performance of a Matrix Air Heater, *Energy Res, 6* (1982), 2, pp. 103-110

Paper submitted: October 15, 2013
Paper revised: June 26, 2014
Paper accepted: June 28, 2014